Dettmann, C. P., Georgiou, O., & Coon, J. P. (2016). More is less: Connectivity in fractal regions. In 2015 International Symposium on Wireless Communication Systems (ISWCS). (pp. 636-640). (Proceedings of the IEEE International Symposium on Wireless Communication Systems (ISWCS)). Institute of Electrical and Electronics Engineers (IEEE). DOI: 10.1109/ISWCS.2015.7454425

More is less: Connectivity in fractal regions

Carl P. Dettmann
School of Mathematics
University of Bristol
Bristol, UK, BS8 1TW
Carl.Dettmann@bristol.ac.uk

Orestis Georgiou
Toshiba Telecommunications Research Laboratory
32 Queens Square
Bristol, UK, BS1 4ND
Orestis.Georgiou@toshiba-trel.com

Justin P. Coon
Department of Engineering Science
University of Oxford
Oxford UK, OX1 3PJ
Justin.Coon@eng.ox.ac.uk

***Abstract*—Ad-hoc networks are often deployed in regions with complicated boundaries. We show that if the boundary is modeled as a fractal, a network requiring line of sight connections has the counterintuitive property that increasing the number of nodes decreases the full connection probability. We characterise this decay as a stretched exponential involving the fractal dimension of the boundary, and discuss mitigation strategies. Applications of this study include the analysis and design of sensor networks operating in rugged terrain (e.g. railway cuttings), mm-wave networks in industrial settings and vehicle-to-vehicle/vehicle-to-infrastructure networks in urban environments.**

I. Introduction

Ad-hoc networks, relying on multihop connections between wireless nodes rather than direct connection to a central router, are of growing importance in both mobile (eg vehicular) and static (eg sensor) networks [1]. Advantages include scalability, flexibility and rapid deployment, as well as energy efficiency and reduced interference associated with lower power transmission. In many applications the spatial region where the nodes are located, an urban mesh wifi network [2], large industrial complex [3], or sensors monitoring a specific geographical feature [4], is highly complex, with boundary features at many length scales.

One of the most successful and long standing models of ad hoc networks is the random geometric graph, where nodes are placed randomly in a region and connect pairwise if they are within a fixed range r_0 (although probabilistic, "soft" connection rules have become popular recently [5]–[7]). There are many mathematical results, in particular, quantifying the rate at which the node density must increase if $r_0 \to 0$ and the full network is to remain connected [8]–[11].

In these studies, the connection region has piecewise smooth boundaries and is typically a torus or square. Rather more general boundaries are considered in Refs. [5], [12] where it is shown how to accurately determine the full connection probability P_{fc} using contributions from boundary components (corners, edges, faces), any of which may dominate depending on the node density. For example, at the highest node densities, the dominant contribution to the outage (lack of connection) probability arises from the sharpest corners, at which the probability of isolated nodes is greatest. Non-convex geometries have also been studied involving connecting through small openings [13], [14] and in the presence of impenetrable obstacles [15]. These studies highlight the important effects of boundaries however become increasingly more difficult to analyse as the complexity of the borders increases.

978-1-4673-6540-6/15/$31.00

Here we make the leap to the extreme case where the network operation region is so complex which can be modelled as a fractal boundary, that is, curves of dimension greater than one (see below for more precise definitions). Fractal models have been used for natural features, for example coastlines (the "Richardson effect", in which the observed length grows significantly as the measuring accuracy improves) as popularised by Mandelbrot [16], as well as other geological features such as mountains and rivers [17], [18]. Fractal boundaries have also been used to describe biological systems, for example trees and lungs [19]. The appearance of fractal structures can be seen a consequence of complex dynamics as in the geological examples, or of optimisation of geometrical parameters, for example maximum surface area at fixed volume, in biology. Both of these are mirrored in the built environment, as fractals also provide a useful model of urban infrastructure including land use and transport networks [20].

One particularly timely application is to sensor networks in the rail industry, to identify age-related deterioration of tracks or emergency conditions due to overloading, natural disasters or sabotage [21]. In this case boundaries are determined by the fractal terrain [17], and a line of sight (LOS) is required for connection. Complicated boundaries and LOS requirements are also relevant to mm-wave networks in large industrial complexes and vehicular networks in urban environments. The ubiquity of fractals suggests fractals with a LOS requirement will be relevant to many other scenarios in the future.

In random geometric graphs with smooth boundaries, the full connection probability increases with node density at moderate and higher densities [5]. But here, it actually *decreases*. Briefly, increased node density leads to a higher probability that one or more very small sub-regions contain a single node that cannot make an LOS connection to any others. The purpose of this paper is to quantify this effect, and propose steps to mitigate it. As a first investigation of the effects of fractal boundaries, and in order to understand the relevant effects without confounding factors, we here restrict consideration to fractal boundaries that are exactly self-similar.

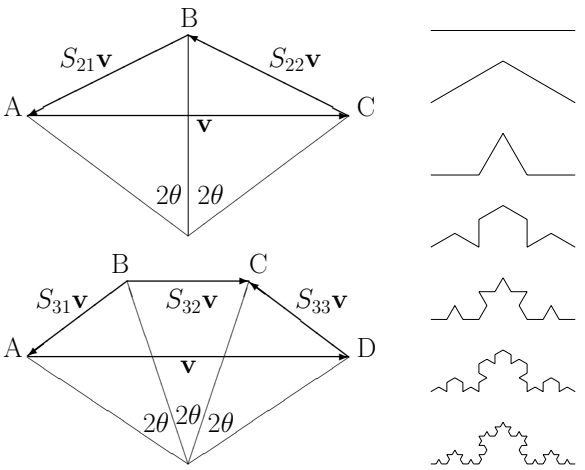

Fig. 1: Left: Similarity transformations defined by their action on the directed line segment $\mathbf{v}$. Points A, B, C and D lie on a circle, subtending angle 2θ from the centre. Right: Construction of $\tilde{F}_2(\pi/6)$ (Koch curve) by repeated action of S_{21} and S_{22} on $\mathbf{v}$.

II. Fractal boundaries

There are many variants on the definition of a fractal, and of fractal dimension [22]. Generally there is some requirement for structures that repeat at many different length scales (though in real systems the range of scales is finite), and that a fractal (eg Hausdorff) dimension is strictly greater than the topological dimension (here 1). We do not need precise definitions of fractal dimensions here; for completeness note that Hausdorff dimension is defined using coverings of the set by boxes of differing sizes while box dimension is defined using boxes of equal size. Box dimension is always greater than or equal to Hausdorff dimension.

The examples we consider are exactly self-similar, so we can define the "similarity dimension" D, the solution of

$$\sum_{i=1}^{n} r_i^D = 1 \tag{1}$$

Here, a fractal set F is defined as the unique non-empty compact set satisfying $F = \cup_{i=1}^{n} S_i F$ where the n similarity transformations S_i (combinations of dilations, rotations, reflections and translations) have dilation factors $0 < r_i < 1$. We also assume here the "open set condition", that is, there is an open set U so that all $S_i U$ are contained in U and are disjoint. That is, the $S_i F$ do not overlap "too much." Then, the Hausdorff and box dimensions are both equal to D [22].

We construct two families of self-similar fractals, denoted $F_2(\theta)$ with $0 < \theta < \pi/4$ and $F_3(\theta)$ with $0 < \theta < \pi/6$. Let points A, B, C and D lie on a circle such that the arcs AB, BC and CD each subtend angle 2θ from the centre. In two dimensions, similarity transformations with no reflections may be uniquely defined by their action on two points. $\tilde{F}_2$ is defined by the transformations S_{21} that maps $A \to B$ and $C \to A$ while S_{22} maps $A \to C$ and $C \to B$. $\tilde{F}_3$ is defined by the transformations S_{31} that maps $A \to B$ and $D \to A$, S_{32} maps $A \to B$ and $D \to C$ and S_{33} maps $A \to D$ and $D \to C$. See Fig. 1. Then, the base interval (directed line segment AC for F_2 or AD for F_3) is transformed to coincide with the interval joining $(-1, 1)$ and $(1, 1)$. Finally, the fractal curve is rotated by multiples of $\pi/2$ about the origin so that it encloses a finite area. The union of the four copies of $\tilde{F}_2$ will be denoted F_2 and similarly with F_3.

For $\theta = 0$, both "fractals" are actually squares of side length 2 and boundary of dimension 1. $\tilde{F}_2(\pi/6)$ is the usual Koch curve constructed by adding an equilateral triangle to the middle third of an initial interval and repeating. $\tilde{F}_2(\pi/5)$ is the "5-fold" Koch curve [23]. In the limit $\theta \to \pi/4$ the curve $\tilde{F}_2$ becomes space filling and of dimension 2. Similarly, in the limit $\theta \to \pi/6$, the curve $\tilde{F}_3$ approaches a Sierpinsky triangle, of dimension $\ln 3/\ln 2 \approx 1.585$.

For both F_n examples and arbirary θ, the scale factors r_i are equal and given by $r = \frac{\sin\theta}{\sin n\theta}$. Direct application of Eq. (1) gives

$$D(F_2(\theta)) = \frac{\ln 2}{\ln(2\cos\theta)} \tag{2}$$

$$D(F_3(\theta)) = \frac{\ln 3}{\ln(4\cos^2\theta - 1)} \tag{3}$$

We can also calculate the area enclosed by each fractal (denoted V for consistency with previous work [5]). We have in both cases $V = 4 + 4V_n(\theta)$ where the first 4 comes from the inner square and $V_n(\theta)$ the area enclosed between $y = 1$ (the horizontal line passing through A) and $\tilde{F}_n$. In each case, we use the similarity transformation and the area of the relevant polygon:

$$V_2(\theta) = \text{Area}(ABC) - 2r^2 V_2(\theta) \tag{4}$$

$$V_3(\theta) = \text{Area}(ABCD) - r^2 V_3(\theta) \tag{5}$$

where in the second case, there are two negative and one positive contributions of $r^2 V_3(\theta)$. Thus

$$V_2(\theta) = \frac{\tan\theta}{1+2r^2} = \frac{\sin(2\theta)}{2+\cos(2\theta)} \tag{6}$$

$$V_3(\theta) = \frac{2\sin^3(2\theta)}{\sin^2(3\theta)}\frac{1}{1+r^2} = \frac{2\sin^3(2\theta)}{\sin^2(3\theta)+\sin^2\theta} \tag{7}$$

For F_2, $4 < V < 6$, while for F_3, $4 < V < \frac{20+12\sqrt{3}}{5} \approx 8.157$.

III. Network connectivity

Nodes are then placed according to a Poisson point process with density ρ inside the fractal (hence expected number of nodes ρV), and pairwise connected if they are within range $r_0 = 1$ and have a line of sight connection. Numerically, this requires two related algorithms. The first and simplest is to test whether a point is inside the fractal. After locating the point in one of the four quadrants defined by $|x| = |y|$ and rotating to the top quadrant, the point lies within the region if $y < 1$ and lies outside if $y > y_{max} = 1 + \tan[(n-1)\theta]$, the highest point on the fractal. Otherwise the appropriate inverse similarity transformations are performed until one of

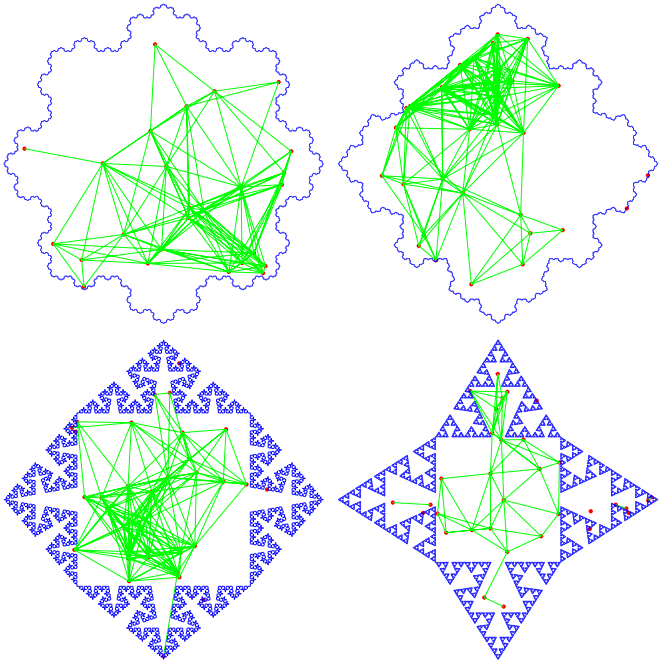

Fig. 2: Typical networks ($\rho = 5$). Left column: $F_2(0.4)$ (top) and $F_2(0.7)$ (bottom). Right column: $F_3(0.3)$ (top) and $F_3(0.5)$ (bottom). Dimensions as found from Eqs. (2, 3) are 1.13, 1.63, 1.13, 1.50 respectively.

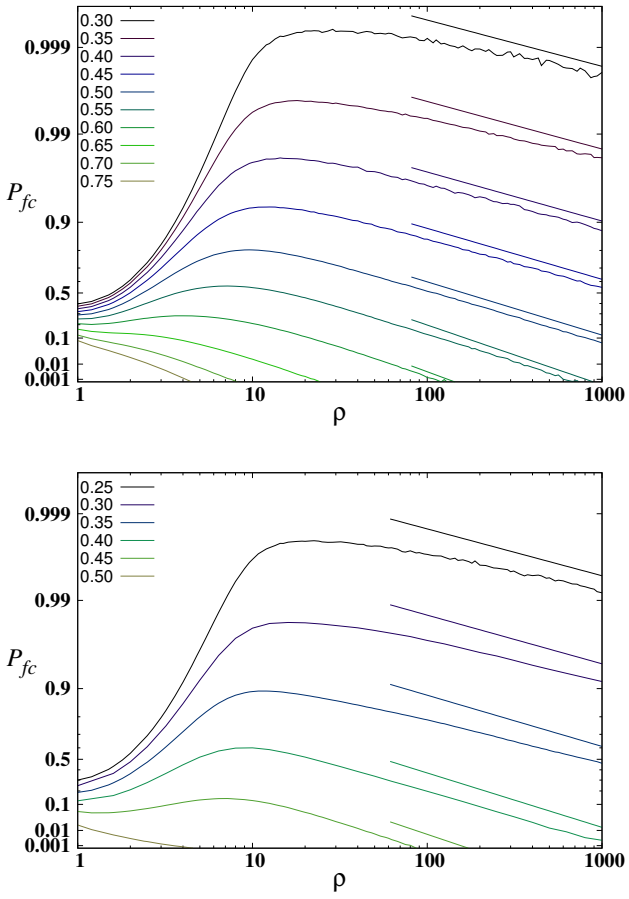

Fig. 3: Full connection probability for $F_2(\theta)$ (top) and $F_3(\theta)$ (bottom) fractals as a function of node density ρ, for values of θ shown in the key. The horizontal axis is logarithmic and the vertical axis double logarithmic, so that Eq. 12 predicts straight lines of slope $D/2$ for high density, which are given for comparison.

these conditions is met, noting that all except S_{32} switch the orientation (that is, move inside points outside and vice versa). The other algorithm is line of sight, tested by recursively applying the inverse similarity transformation on the whole line segment between the two nodes. If the line segment crosses the boundaries of the transformation regions, it is split into smaller sections. The test is for whether the interval intersects the fractal (yes if it has one endpoint with $y < 1$ and one with $y > y_{max}$, no if both end points satisfy one of these conditions), so no orientation information needs to be retained. Typical networks constructed in this manner are shown in Fig. 2.

Here, we are concerned with the probability of full connectivity, P_{fc}, the fraction of possible node configurations in which all nodes are connected in a multihop fashion, and hence ensure low latency communications throughout the network. To determine the effect of high node density ρ on connectivity, we neglect for now the possibility of nodes not closer than the finite range r_0 and consider the line of sight effects near the fractal boundary. Observe that by increasing density by a factor r^{-d} leads to the same distribution of nodes one iteration further into the fractal, where $d = 2$ is the dimension of the ambient space. There are n equivalent regions, each with a probability similar to the original of disconnecting due to an isolated node near the boundary. Thus we have for large node density

$$P_{fc}(r^{-d}\rho) = P_{fc}(\rho)^n \tag{8}$$

Taking logarithms we see that multiplying ρ by the factor r^{-d} leads to $-\ln P_{fc}$ increasing by a factor n. Thus we expect $-\ln P_{fc}$ to grow algebraically with ρ. This motivates the substitution

$$P_{fc} = \exp[-a(\rho)\rho^\beta] \tag{9}$$

with $a(\rho)$ and β as yet undetermined. Eq. (8) reduces to

$$a(r^{-d}\rho)r^{-d\beta} = na(\rho) \tag{10}$$

Substituting Eq. 1 and choosing $\beta = D/d$ we have simply

$$a(r^{-d}\rho) = a(\rho) \tag{11}$$

Thus the coefficient a is an unknown periodic function of $\ln \rho$ with period $d \ln r^{-1}$. In principle we could expand it in a

Fourier series, however, we expect that connection probability is a smooth function of density, so we expect it to be dominated by its leading constant term [24]. We will henceforth treat it as constant, leading to our main result

$$P_{fc} = \exp[-a\rho^{D/d}] \tag{12}$$

Thus we expect a stretched exponential decay of connection probability with density, in contrast to smooth boundaries for which $P_{fc} \to 1$ exponentially fast. Relevant numerical simulations are presented in Fig. 3. For comparison, straight lines corresponding to Eq. (12) are included. Here, the value of a was arbitrarily chosen since the primary purpose of the illustration is to demonstrate the slope of the connectivity probability decay. Further analysis of this parameter is not considered in the present contribution. Notably, there is good agreement whether the ordinate $-\ln(-\ln P_{fc})$ is positive or negative, that is, P_{fc} is close to one or zero, respectively.

IV. Discussion and further applications

We now discuss and generalise some assumptions made in the above argument. First, some of the transformations for $F_2(\theta)$ and $F_3(\theta)$ invert the orientation of the curve, so that features that are inside the domain move outside the domain and vice versa. For $F_2(\theta)$ both transformations invert, so we may simply apply the transformation twice, yielding the same stretched exponential. In $F_3(\theta)$ the number of accessible outer regions at level m is $2 \times (3^m + (-1)^m)$ and so the ratio of accessible regions still approaches $n = 3$ in the relevant limit (high density). Similarly, for more general fractals with differing (and generally multiplicatively incommensurate) scale factors r_i, or for fractals that are only statistically self-similar, the scaling argument may apply in an average sense, giving again Eq. (12).

The above analysis also applies to more complicated local network features. For example, consider localisation of a robot swarm [25]. Starting from three nodes with known locations, any node connected to at least three localisable nodes is localisable (in two dimensions), the trilateration algorithm. Whether any node is connected to three closer to the large component is a scale invariant quantity, and so the above argument carries through, giving the same stretched exponential with a larger value of a. This applies also to more sophisticated algorithms involving larger (but still local) network structures such as wheels [26].

As we have seen, the fractal boundary leads to a reduction in connection probability at high node densities. At lower densities, we see from Fig. 3 that the connection probability increases with density (that is, it is not monotonic). For densities that are not too small, this is almost entirely due to isolated nodes in the interior, as discussed by many previous authors [5], [8]–[11]. Given the Poisson distribution, it is easy to see that for a given node, the probability that no node lies in a circle of radius r_0 around it is $\exp[-\rho\pi r_0^2]$. Such events can be shown to be almost independent, so the expected number of isolated nodes in the interior is $\rho V \exp[-\rho\pi r_0^2]$. However, there are many regions near the boundary for which the full area πr_0^2 is not available; a detailed analysis is likely to be complicated and deferred to a future paper. Qualitatively we see that there is a density at which connectivity is maximised. Increasing the connection range r_0 decreases the optimum density while increasing the maximum probability. However, this will come at a cost to energy consumption.

Strictly speaking, the infinite density limit is singular - while our argument holds for arbitrarily large finite densities, an infinite number of nodes placed with respect to any translationally invariant random process is connected, since the set of nodes is dense. So, there are no isolated nodes. Truly infinite densities are of theoretical interest only, however, physical constraints will place a lower limit on the relevant length scales. At sufficiently small scales, the boundary will be smooth, the nodes will be able to communicate through it, and size of the nodes themselves will prevent their approaching the boundary too closely. All of these mean that at sufficiently high node densities (of the order of $\epsilon^{-d} \ln \epsilon$, where ϵ is the relevant very small length scale) connectivity will be regained. The number of nodes required, however is prohibitively expensive compared with the few needed for geometries with smooth boundaries, since $\epsilon \ll r_0$.

The most resource efficient approach to regaining connectivity is likely to be the placement of gateway nodes near the entrances to the fractal lobes. The number of such nodes required to cover the fractal boundary is proportional to the typical length scale $\rho^{-1/d}$ to the fractal exponent D, that is, the power $\rho^{-D/d}$ appearing in the stretched exponential. This is much smaller that the total number of nodes (on average $V\rho$). However, this approach suffers from having to know the shape of the (often time-dependent) boundary in great detail.

We illustrate the preceding arguments for a vehicular ad-hoc network in an urban environment. The dimension of an urban transport network varies significantly, but is typically around 1.25 [27]. Assuming an overall scale of 10^4m and boundary roughness down to 100m, we need roughly $(10^4/10^2)^2 = 10^4$ nodes to ensure complete coverage, but only $(10^4/10^2)^{1.25} \approx 316$ gateway nodes (in this case, static roadside units [28]).

V. Conclusion

We have analysed the connectivity of dense networks confined to regions with fractal boundaries, finding a surprising result: Increasing the density of nodes leads to lower probability of full connectivity. We have quantified this in terms of a stretched exponential involving fractal dimension D and confirmed this numerically for two families of self-similar fractals.

It is important to know how these effects generalise to more general complex geometries, for example self-affine or statistically self-similar fractals, and also the effect of complex boundaries on global network properties of relevance to wireless applications, such as centrality measures [29].

We discussed a number of generalisations and amelioration strategies, however these require a very high outlay of nodes and/or detailed knowledge of the fractal boundary. It is likely therefore that lack of connectivity for networks in complicated

geometries will be an increasingly significant issue in the future.

ACKNOWLEDGMENTS

The authors would like to thank Shinichi Baba, Jonathan Fraser, Thomas Jordan, Jed Keesling and Bill Mance for helpful discussions and the directors of the Toshiba Telecommunications Research Laboratory for their support. JPC and OG would like to acknowledge the support of the European Commission partly funding the DIWINE project under Grant Agreement CNET-ICT-318177.

REFERENCES

[1] C. de Morais Cordeiro and D. P. Agrawal, *Ad hoc and sensor networks: theory and applications*. World Scientific, 2011.

[2] S. Vural, D. Wei, and K. Moessner, "Survey of experimental evaluation studies for wireless mesh network deployments in urban areas towards ubiquitous internet," *Communications Surveys & Tutorials, IEEE*, vol. 15, no. 1, pp. 223–239, 2013.

[3] S. Savazzi, U. Spagnolini, L. Goratti, and S. Galimberti, "Wireless cloud networks for critical industrial quality control," in *Wireless Communication Systems (ISWCS 2013), Proceedings of the Tenth International Symposium on*. VDE, 2013, pp. 1–5.

[4] F. Ingelrest, G. Barrenetxea, G. Schaefer, M. Vetterli, O. Couach, and M. Parlange, "Sensorscope: Application-specific sensor network for environmental monitoring," *ACM Transactions on Sensor Networks (TOSN)*, vol. 6, no. 2, p. 17, 2010.

[5] J. Coon, C. P. Dettmann, and O. Georgiou, "Full connectivity: corners, edges and faces," *J. Stat. Phys.*, vol. 147, no. 4, pp. 758–778, 2012.

[6] M. D. Penrose, "Connectivity of soft random geometric graphs," *Ann. Appl. Prob. (to appear); arXiv:1311.3897*, 2013.

[7] M. Haenggi, J. G. Andrews, F. Baccelli, O. Dousse, and M. Franceschetti, "Stochastic geometry and random graphs for the analysis and design of wireless networks," *IEEE J. Select. Areas Comm.*, vol. 27, no. 7, pp. 1029–1046, 2009.

[8] M. D. Penrose, "The longest edge of the random minimal spanning tree," *Ann. Appl. Prob.*, pp. 340–361, 1997.

[9] P. Gupta and P. R. Kumar, "Critical power for asymptotic connectivity in wireless networks," in *Stochastic analysis, control, optimization and applications*. Springer, 1999, pp. 547–566.

[10] M. Walters, "Random geometric graphs," *Surveys in Combinatorics*, vol. 392, pp. 365–402, 2011.

[11] G. Mao and B. Anderson, "Towards a better understanding of large-scale network models," *IEEE/ACM Transactions on Networking (TON)*, vol. 20, no. 2, pp. 408–421, 2012.

[12] J. P. Coon, O. Georgiou, and C. P. Dettmann, "Connectivity in dense networks confined within right prisms," in *Proceedings of SPASWIN 2014: International workshop on spatial stochastic models for wireless networks*, 2014.

[13] O. Georgiou, C. P. Dettmann, and J. P. Coon, "Network connectivity through small openings," in *Proc. ISWCS 2013*. VDE, 2013, pp. 1–5.

[14] O. Georgiou, M. Z. Bocus, M. R. Rahman, C. P. Dettmann, and J. P. Coon, "Network connectivity in non-convex domains with reflections," *IEEE Commun. Lett.*, vol. 19, pp. 427–430, 2015.

[15] A. Giles, O. Georgiou, and C. P. Dettmann, "Connectivity of soft random geometric graphs over annuli," *arXiv:1502.05440*, 2015.

[16] B. B. Mandelbrot, "How long is the coast of Britain?" *Science*, vol. 156, no. 3775, pp. 636–638, 1967.

[17] P. Prusinkiewicz and M. Hammel, "A fractal model of mountains and rivers," in *Graphics Interface*, vol. 93. Canadian Information Processing Society, 1993, pp. 174–180.

[18] D. L. Turcotte, *Fractals and chaos in geology and geophysics*. Cambridge University Press, 1997.

[19] G. A. Losa, "Fractals in biology and medicine," *Encycl. Mol. Cell Biol. Mol. Med.*, 2011.

[20] G. Shen, "Fractal dimension and fractal growth of urbanized areas," *Intl.J. Geog. Inform. Sci.*, vol. 16, no. 5, pp. 419–437, 2002.

[21] V. J. Hodge, S. O'Keefe, M. Weeks, and A. Moulds, "Wireless sensor networks for condition monitoring in the railway industry: A survey," *Intell. Transport Sys., IEEE Trans.*, 2014.

[22] K. Falconer, *Fractal geometry: mathematical foundations and applications*. John Wiley & Sons, 2013.

[23] C. P. Dettmann and N. E. Frankel, "Structure factor of deterministic fractals with rotations," *Fractals*, vol. 1, no. 02, pp. 253–261, 1993.

[24] ——, "Potential theory and analytic properties of a Cantor set," *Journal of Physics A: Mathematical and General*, vol. 26, no. 5, p. 1009, 1993.

[25] J. C. Barca and Y. A. Sekercioglu, "Swarm robotics reviewed," *Robotica*, vol. 31, no. 03, pp. 345–359, 2013.

[26] Z. Yang, Y. Liu, and M. Li, "Beyond trilateration: On the localizability of wireless ad-hoc networks," in *INFOCOM 2009, IEEE*. IEEE, 2009, pp. 2392–2400.

[27] Y. Lu and J. Tang, "Fractal dimension of a transportation network and its relationship with urban growth: a study of the dallas-fort worth area," *Environment and Planning B*, vol. 31, pp. 895–912, 2004.

[28] S. Al-Sultan, M. M. Al-Doori, A. H. Al-Bayatti, and H. Zedan, "A comprehensive survey on vehicular ad hoc network," *Journal of network and computer applications*, vol. 37, pp. 380–392, 2014.

[29] A. Jain and B. Reddy, "Node centrality in wireless sensor networks: Importance, applications and advances," in *Advance Computing Conference (IACC), 2013 IEEE 3rd International*. IEEE, 2013, pp. 127–131.